


# Chronic everolimus treatment of high-fat diet mice leads to a reduction in obesity but impaired glucose tolerance

Geng-Ruei Chang<sup>1</sup>  | Po-Hsun Hou<sup>2,3</sup> | Chao-Min Wang<sup>1</sup> | Ching-Feng Wu<sup>4</sup> | Huang-Kai Su<sup>1</sup> | Huei-Jyuan Liao<sup>1</sup> | To-Pang Chen<sup>5</sup>

<sup>1</sup>Department of Veterinary Medicine, National Chiayi University, Chiayi, Taiwan

<sup>2</sup>Department of Psychiatry, Taichung Veterans General Hospital, Taichung, Taiwan

<sup>3</sup>Faculty of Medicine, National Yang-Ming University, Taipei, Taiwan

<sup>4</sup>Division of Thoracic and Cardiovascular Surgery, Department of Surgery, Chang Gung University, Chang Gung Memorial Hospital, Taoyuan, Taiwan

<sup>5</sup>Division of Endocrinology and Metabolism, Show Chwan Memorial Hospital, Changhua, Taiwan

## Correspondence

Geng-Ruei Chang, Department of Veterinary Medicine, National Chiayi University, 580 Xinmin Road, Chiayi 60054, Taiwan.

Email: grchang@mail.ncyu.edu.tw

To-Pang Chen, Division of Endocrinology and Metabolism, Show Chwan Memorial Hospital, 1 Section, 542 Chung-Shan Road, Changhua 50008, Taiwan.  
Email: s881055@gmail.com

## Funding information

Ministry of Education, Executive Yuan, Grant/Award Number: 109D1-100A-A-A2; Show Chwan Memorial Hospital, Grant/Award Number: SRD108025; Chang Gung Memorial Hospital, Grant/Award Number: CMRPG5J0191; Taichung Veterans General Hospital; National Chung-Hsing University, Grant/Award Number: TCVGH-NCHU-1097612; National Chiayi University, Grant/Award Number: 108A3-129, 108A3-147 and 108A3-161

## Abstract

Everolimus, which inhibits mTOR kinase activity and is clinically used in graft rejection treatment, may have a two-sided influence on metabolic syndrome; its role in obesity and hyperglycemic in animals and humans, however, has been explored insufficiently. This study further determined how continual everolimus treatment affects glucose homeostasis and body weight control in C57BL6/J mice with obesity. An obesity mouse model was developed by administering a high-fat diet (HFD) to C57BL6/J mice over 12 weeks. The experimental group, while continuing their HFD consumption, were administered everolimus daily for 8 weeks. Metabolic parameters, glucose tolerance, fatty liver score, endocrine profile, insulin sensitivity index (ISI), insulin resistance (IR) index, and Akt phosphorylation, GLUT4, TNF- $\alpha$ , and IL-1 levels were measured in vivo. Compared with the control group, the everolimus group gained less body weight and had smaller adipocytes and lower fat pad weight; triglyceride (serum and hepatic), patatin-like phospholipase domain-containing 3, and fatty acid synthase levels; fatty liver scores; and glucose tolerance test values—all despite consuming more food. However, the everolimus group exhibited decreased ISI and muscle Akt phosphorylation and GLUT4 expression as well as impaired glucose tolerance and serum TNF- $\alpha$  and IL-1 $\beta$  levels—even when insulin levels were high. In conclusion, continual everolimus treatment may lead to diabetes with glucose intolerance and IR.

## KEYWORDS

adipocyte, everolimus, glucose intolerance, insulin sensitivity, obesity

**Abbreviations:** AMPK, adenosine monophosphate-activated protein kinase; AUC, area under the glucose tolerance curve; EWAT, epididymal white adipose tissue; FA, fatty acid; FASN, fatty acid synthase; FGF21, fibroblast growth factor 21; GLUT4, glucose transporter 4; GTT, glucose tolerance test; HFD, high-fat diet; IL-1 $\beta$ , interleukin-1 $\beta$ ; IPGTT, intraperitoneal GTT; mTOR, mammalian target of rapamycin; PEPCK, phosphoenolpyruvate carboxy kinase; PNPLA3, patatin-like phospholipase domain-containing 3; RWAT, retroperitoneal white adipose tissue; S6K1, S6 ribosomal protein kinase 1; SD, standard diet; TNF- $\alpha$ , tumor necrosis factor- $\alpha$ .

This is an open access article under the terms of the Creative Commons Attribution-NonCommercial-NoDerivs License, which permits use and distribution in any medium, provided the original work is properly cited, the use is non-commercial and no modifications or adaptations are made.

© 2021 The Authors. *Pharmacology Research & Perspectives* published by John Wiley & Sons Ltd, British Pharmacological Society and American Society for Pharmacology and Experimental Therapeutics and John Wiley & Sons Ltd.

## 1 | INTRODUCTION

The new-generation mammalian target of rapamycin (mTOR) inhibitor everolimus is widely used as an antirejection drug in patients undergoing organ transplantation.<sup>1</sup> In mammalian cells, mTOR exists in two forms that differ in structure and physical function: mTORC1 and mTORC2. The overexpression or mutation relating to this pathway is central in the tumorigenesis of various cancer types including renal cell cancers, pancreatic tumors, and gastrointestinal, lung, and hormone-related breast cancers.<sup>2</sup> Moreover, everolimus directly inhibits the mTORC1 complex involved in the mTORC1-S6 K1 signaling pathway, which regulates the nutritional status and in turn regulates cellular- and organismal-level energy homeostasis including protein and lipid synthesis and adipogenesis.<sup>3-5</sup> Energy homeostasis is majorly involved in neurological disorders, cardiovascular diseases, obesity, and diabetes.<sup>6</sup> Moreover, increased mTOR activity was demonstrated to be associated with insulin resistance (IR)<sup>7</sup> and treatment with an mTOR inhibitor was shown to result in increased insulin sensitivity (IS) and glucose uptake.<sup>8</sup>

Type 2 DM, in which  $\beta$ -cell hypersecretion cannot overcome the IR of target tissue, is widespread in developed countries and has a strong correlation with obesity.<sup>9-11</sup> In a human fibroblast cell study, leucine directly stimulated mTORC1-dependent phosphorylation signaling after a short period of amino acid starvation, indicating that the mTOR pathway is closely involved in cellular amino acid regulation, gluconeogenesis, and metabolism.<sup>12</sup> Moreover, inhibition of mTOR pathway activity decreased lipogenesis, and adipogenesis through lipid metabolism involves lipoprotein scavenging, lipid oxidation, and ketogenesis.<sup>13</sup> Overall, these results suggest inhibition of mTOR signaling as a strategy for reducing adiposity and preventing obesity and type 2 DM complications including cardiomyopathy, it was also demonstrated to protect mice against obesity induced by a high-fat diet (HFD).<sup>14,15</sup>

Because promising results have been obtained in clinical studies,<sup>1</sup> everolimus, both alone and in tandem with endocrine or antiangiogenic agents, is presently being assessed for treatment in hematological, neuroendocrine, colorectal, renal, and lung tumors. In addition, studies have demonstrated that the common adverse events occurring during everolimus treatment are hyperglycemia and hyperlipidemia, with triglyceride levels being elevated,<sup>3</sup> and that everolimus induced hyperlipidemia through disruption of cellular lipid homeostasis in mice.<sup>16</sup> Hyperglycemia is a major side effect, however, some clinical studies indicated that hyperglycemia is less likely to occur for immunosuppressant use rather than anticancer use of everolimus.<sup>17,18</sup> In contrast, some clinical studies have reported that although the levels of fasting blood glucose became significantly lower after everolimus treatment, the changes in triglyceride, cholesterol, blood magnesium, and uric acid levels; body mass index; body weight; and lipid-lowering medication requirements were nonsignificant.<sup>19,20</sup> Everolimus treatment prevented high-cholesterol fructose-induced steatosis and improved metabolic parameters, such as IR and dyslipidemia, in mice.<sup>21</sup> These findings

suggest that everolimus does not negatively influence various nutritional parameters.

Because everolimus selectively inhibits mTOR signaling in body-wide cells, considering the effect on glucose homeostasis in peripheral tissues is as crucial as considering the insulin-related mechanisms. However, consistent with the aforementioned notion of a two-sided influence on metabolic syndrome, the differences among the reported effects of everolimus in the discussions of the everolimus-related hyperglycemia pathogenesis are probably caused by differences induced by metabolic syndrome and nonmetabolic syndrome. We sought to determine whether continual everolimus treatment in obese animals with hyperglycemia would affect the animals' body weight, blood glucose, lipid values, insulin signaling expression, endocrine profile, and fatty liver status, which is a syndrome influencing lipid metabolism and exerts more adverse effects in people who have obesity, DM, glucose intolerance, and atherosclerosis.<sup>10,14</sup> Furthermore, we examined the influence of everolimus on glucose homeostasis in addition to insulin-related mechanisms by performing glucose tolerance tests (GTTs) and determining pancreatic  $\beta$ -cell function and IR indices; these approaches are common in DM studies and suitable for metabolomic analysis.

## 2 | MATERIALS AND METHODS

### 2.1 | Animals and drug treatment

We acquired C57BL/6J mice (age: 5 weeks; sex: male) from the Education Research Resource, National Laboratory Animal Center, Taiwan and performed all animal experimentation in accordance with the Taiwan government's Guidelines for the Care and Use of Laboratory Animals and with the approval of National Chiayi University's Institutional Animal Care and Use Committee (approval No.: 109019).

The standard diet (SD) was diet 5008 (composed of 24% protein and 49.4% carbohydrates) purchased from PMI Nutrition International). This SD given to all mice for 2 weeks. Thereafter, for 12 weeks, all mice were fed an HFD: diet 592Z (a 20.4% protein-enriched diet modified with 35.5% lard) from PMI Nutrition International. All feeding was ad libitum. Four weeks of an HFD are generally required to achieve a diet-induced obesity model.<sup>22,23</sup> All mice were kept in the animal quarters, here, each mouse was provided an individual microisolation cage, which was placed on racks ventilated using high-efficiency particulate air filters (Rungshin IVC Systems). In the quarters, we applied a 12:12-h light-dark cycle, while maintaining the temperature at  $22^{\circ}\text{C} \pm 1^{\circ}\text{C}$  and humidity at  $55\% \pm 5\%$ . The food intake and body weight of each mouse was measured weekly.

The mice fed a 12-week HFD had higher body weight (HFD  $38.74 \pm 0.58$  g vs. SD  $26.17 \pm 0.41$  g,  $p < 0.001$ ), fasting blood glucose level (HFD  $7.23 \pm 0.18$  mmol/L vs. SD  $4.75 \pm 0.39$  mmol/L,  $p < 0.01$ ), and triglyceride level (HFD  $1.81 \pm 0.13$  mmol/L vs. SD  $0.97 \pm 0.08$  mg/dL,  $p < 0.01$ ) than did the SD-fed mice ( $n = 20$  for all groups), following

up our preliminary investigation. At the age of 19 weeks, we randomly divided the obese mice into HFD control (mass:  $38.64 \pm 0.96$  g) and everolimus (mass:  $38.84 \pm 0.85$  g) groups, without significant between-group differences. The everolimus group received an intraperitoneal (i.p.) everolimus injection (1.5 mg/kg body weight) once daily for 56 days while remaining on the HFD. The HFD control group were administered the corresponding volume of the vehicle (8% ethanol, 10% PEG 400, and 10% Tween 80).<sup>24</sup> The everolimus dose was selected according to the literature regarding the use of everolimus as a candidate for chronic treatment in metastatic breast cancer, atherosclerosis, xenograft, heart transplantation, hypercholesterolemia, and endometriotic studies in a mouse model.<sup>25–30</sup>

## 2.2 | Body weight, tissue and organ weight, food intake, as well as serum hormone, fatty acid, fibroblast growth factor 21, interleukin 1 $\beta$ , and tumor necrosis factor $\alpha$ level measurement

Every week, we measured the mice's body weights. In addition, we measured the food intake weekly by weighing the food left in each cage including that in each cage's dispenser and floor. After the study period ended, the mice were euthanized, and certain tissues/organs and serum were obtained for analyzing insulin, leptin, fatty acid (FA), fibroblast growth factor 21 (FGF21), interleukin (IL) 1 $\beta$ , and tumor necrosis factor (TNF)  $\alpha$  levels. In addition, the liver and retroperitoneal white adipose tissue (RWAT) and epididymal white adipose tissue (EWAT) pads were extracted and weighed, and all organ weights were expressed as percentages of body weight.

## 2.3 | GTT

After a 56-day treatment with a vehicle or everolimus, we performed an intraperitoneal GTT (IPGTT) by using a 1 g/kg body weight glucose; before the test, the mice were fasted overnight with free access to water. We measured the blood glucose level of the mice at 0, 30, 60, 90, and 120 min after the i.p. injection. Blood levels of glucose were measured using blood from the tail vein on a One Touch glucose meter (LifeScan). We calculated the area under the glucose tolerance curve (AUC) over 0–120 min to identify glucose tolerance.

## 2.4 | Serum triglyceride and hepatic triglyceride level measurement

After the mice were euthanized, we collected blood samples and analyzed their serum triglyceride concentration. Serum triglyceride levels were measured using an IDEXX automated chemistry analyzer (IDEXX Laboratories), in accordance with the manufacturer's instructions. Hepatic triglycerides were extracted using Triton X-100 solution from the homogenized liver samples by employing the procedure of London and Castonguay.<sup>31</sup> Then, the extracted samples were solubilized

through two cycles of gradual heating to 90°C over 5 min followed by cooling to room temperature, this solution was then centrifuged to eliminate insoluble material. The supernatant was finally collected for colorimetric assay-based triglyceride analysis.

## 2.5 | Histological and morphometric analysis

After the animals were killed, the livers, RWAT and EWAT were collected for histopathological examination and scoring. Two slides were selected from each animal, and  $\geq 10$  fields (200 $\times$  magnification) on each slide were randomly selected to evaluate fatty liver changes. In addition, fatty infiltration of the liver was visualized through hematoxylin–eosin staining; liver surface infiltration was rated as 0 (no visible infiltration), 1 (<5% infiltration), 2 (5%–25% infiltration), 3 (25%–50% infiltration), or 4 (>50% infiltration).<sup>6,14</sup>

We collected several sections from RWAT and EWAT pads, and the adipocyte number and size therein were evaluated systematically. Hematoxylin–eosin staining was performed. At least 10 fields (representing nearly 100 adipocytes) on two slides for each sample from each animal were analyzed.<sup>10,23</sup> We captured images through high-resolution digital microscopy (Moticam 2300, Motic Instruments) and determined the adipocyte size distribution on Motic Images Plus (version 2.0). For the HFD control and everolimus groups, adipocyte size correlation and distribution (%) were determined. All sections were reassessed for fatty liver infiltration and adipocyte changes by Taiwan-certified veterinary pathologists blinded to the animals' treatments.

## 2.6 | RNA extraction and real-time quantitative polymerase chain reaction

We used TRI Reagent to extract total RNA from liver tissues. RNA concentration was assessed on the basis of absorbance at 260–280 and 230–260 nm on a Qubit fluorometer (Invitrogen). We then reverse transcribed the RNA (1  $\mu$ g) into cDNA by using an iScript cDNA synthesis kit in accordance with manufacturer instructions. Subsequently, we performed a real-time polymerase chain reaction (PCR) using this cDNA and the iTaq universal SYBR Green supermix in accordance with manufacturer protocol. Phosphoenolpyruvate carboxy kinase (PEPCK) mRNA expression levels were specifically determined using the CFX Connect Real-Time PCR System (Bio-Rad). The PCR was performed as follows: 95°C for 5 min and then 45 cycles at 95°C for 15 s followed by 60°C for 25 s. The PEPCK sequence primers employed in this study were 5'-AACTGTTGGCTGGCTCTC-3' (forward) and 5'-GAACCTGGCGTTGAATGC-3' (reverse<sup>32</sup>).

## 2.7 | Western blot analysis

The mice were anesthetized at the end of each experiment through an i.p. injection; immediately after anesthesia, we

removed the gastrocnemius muscles of the mice and minced them coarsely followed by homogenization. We performed Western blotting as described elsewhere<sup>6</sup> by using the following antibodies: anti-fatty acid synthase (FASN), adiponectin, anti-patatin-like phospholipase domain-containing 3 (PNPLA3), anti-adenosine monophosphate-activated protein kinase (AMPK), anti-Akt, anti-glucose transporter 4 (GLUT4), anti-mTOR, anti-S6K, anti-actin, anti-phospho-AMPK (Thr172), anti-phospho-Akt (Ser473), anti-phospho-mTOR (Ser2448), and anti-phospho-S6K (Thr389). Enhanced chemiluminescence reagents were employed to detect immunoreactive signals, and we exposed the membranes on X-ray film. Protein expression and phosphorylation on films were quantified using the National Institutes of Health program Scion Image.

## 2.8 | IR and IS indices

The homeostasis model assessment (HOMA) can be used to determine the IR index, HOMA-IR, and the IS index (ISI). This method has been validated against clamp measurements. Fasting glucose has been widely used to estimate IR and IS.<sup>23,33</sup> Therefore, these two indices were used to evaluate the posttreatment insulin function and IR of the mice. The HOMA-IR was calculated as follows<sup>6,23</sup>:

$$\text{HOMA-IR} = [\text{fasting insulin (mU/L)} \times \text{fasting glucose (mmol/L)}] / 22.5$$

$$\text{HOMA-IR} = [\text{fasting insulin (mU/L)} \times \text{fasting glucose (mmol/L)}] / 22.5$$

The ISI was computed using the following equation:

$$\text{ISI} = [1/\text{fasting insulin (mU/L)} \times \text{fasting glucose (mmol/L)}] \times 1000.$$

## 2.9 | Statistical analysis

We present results as mean values with the standard errors of the means (SEMs). For two-group comparisons, we used the *t* test, whereas for comparing two or more groups, we employed analysis of variance, followed by post hoc analysis using Bonferroni correction. A *p* of <0.05 was considered to indicate significance. We assessed contingency data's significance by employing Fisher's exact test.

## 2.10 | Other material

We purchased TRI Reagent, everolimus, and the anti-PNPLA3 antibody and colorimetric FA assay kit from Sigma-Aldrich; cDNA synthesis kit and iTaq universal SYBR Green supermix from Bio-Rad; mouse leptin and insulin enzyme-linked immunosorbent assay (ELISA) kits from Crystal Chem; mouse TNF- $\alpha$  and IL-1 $\beta$  ELISA kits from Invitrogen; the BioVision Triglyceride Quantification Kit (a colorimetric assay kit) from BioVision; anti-FASN, anti-phospho-AMPK (Thr172), anti-AMPK, anti-phospho-Akt (Ser473), anti-Akt, anti-GLUT4, anti-phospho-mTOR (Ser2448), anti-mTOR, anti-phospho-S6 K (Thr389), anti-S6 K, and anti-actin antibodies from Cell Signaling Technology; enhanced chemiluminescence reagents from Pierce (Rockford, IL, USA); and FGF21 ELISA kits from Zgenebio Biotech.

## 3 | RESULTS

### 3.1 | Everolimus affects the morphometric parameters, food intake, and food efficiency of obese animals

In our preliminary studies, the body weights and body weight gain of everolimus-treated SD-fed mice did not differ significantly from those of the control SD-fed mice. Thus, we initiated this study by using an HFD-induced obesity mice model (Figure 1). The obese mice that underwent everolimus treatment for 8 weeks exhibited higher morphometric parameters and lower serum leptin levels than did the control mice (Figure 2). The body weights of the HFD everolimus group gradually decreased over 56 days, resulting in mean body weight approximately 20% lower than that of HFD-fed controls (*p* < 0.001; Figure 2A). When the treatment ended, the between-group difference in the body weight change was significant (*p* < 0.001; Figure 2B). The everolimus-treated mice gained 83% less weight each week than did the control group; this difference was significant (*p* < 0.001; Figure 2C). Nonetheless, the everolimus group had significantly increased weekly food intake (*p* < 0.01; Figure 2D). The weekly food efficiency was also lower in the everolimus-treated mice than in the control mice (*p* < 0.001; Figure 2E). Therefore, we could not attribute the lower body weight of the everolimus-treated mice

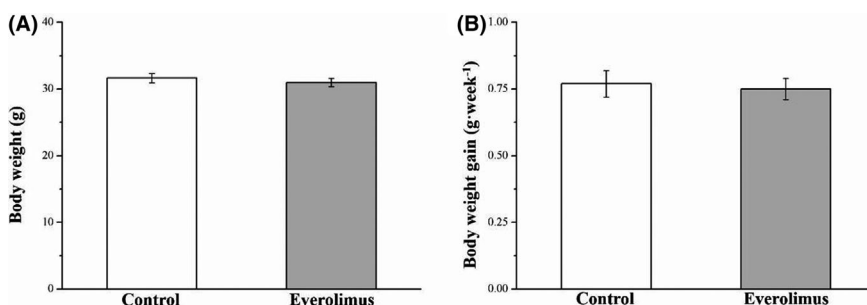


**FIGURE 1** Changes in (A) body weight and (B) weekly body weight gain in the control and everolimus-treated SD-fed mice over 56 treatment days. All values are presented as means  $\pm$  SEMs, and *n* = 10 for all groups

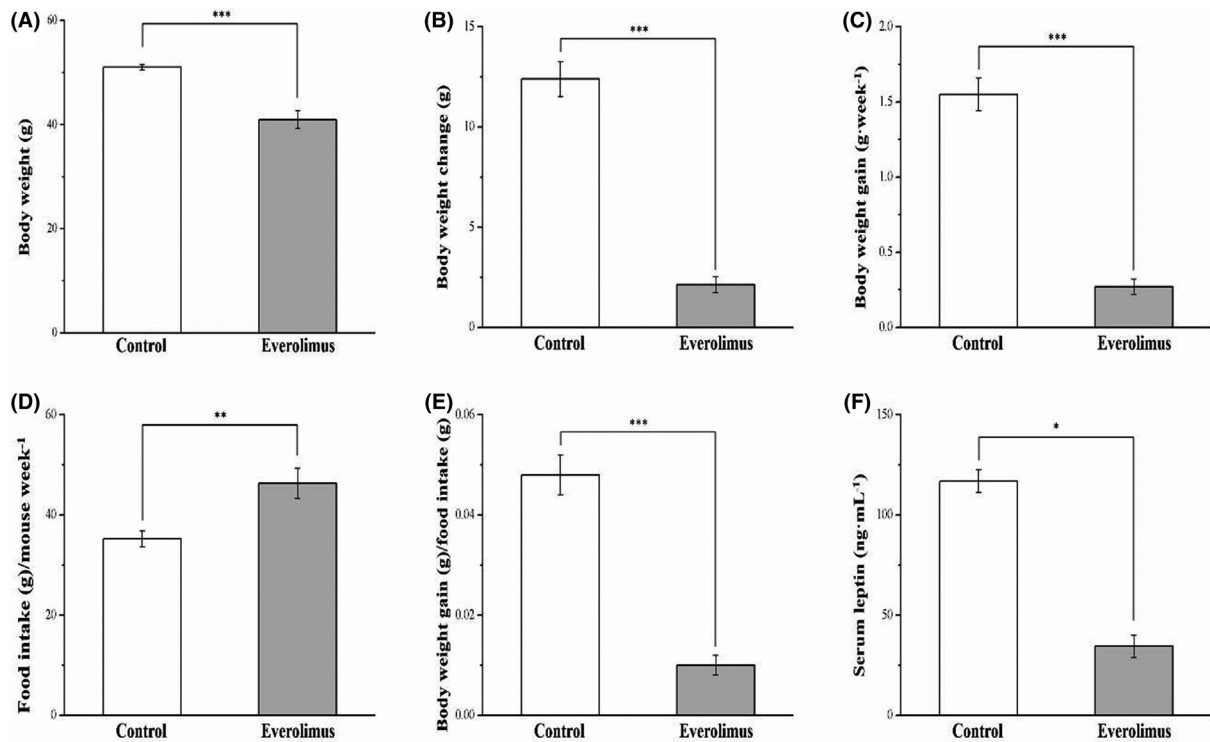


**FIGURE 2** Changes in (A) body weight, (B) body weight change, (C) body weight gain, (D) food intake (per mouse per week), (E) daily food efficiency, and (F) serum leptin level in the control and everolimus-treated HFD-fed mice over 56 treatment days. All values are presented as means  $\pm$  SEMs, and  $n = 10$  for all groups. \* $p < 0.05$ , significant; \*\* $p < 0.01$ , highly significant; \*\*\* $p < 0.001$ , extremely significant

to a lower food intake. Everolimus treatment was discovered to significantly affect serum leptin level ( $p < 0.05$ ), which is known to participate in food intake regulation (Figure 2F). This finding was thus consistent with the food intake result.

### 3.2 | Everolimus reduces liver and fat pad weight

Whether the differences in weight were a result of liver or adiposity alterations was then investigated. The everolimus group, after 8 weeks of everolimus treatment, had body composition significantly different from the control group: the liver, RWAT pad, and EWAT pad weights demonstrated 35%, 37%, and 45% reductions, respectively (all  $p < 0.01$ ; Figure 3). Furthermore, when expressed as percentages of body weight, the liver, RWAT, and EWAT weights were 19% ( $p < 0.05$ ), 32% ( $p < 0.01$ ), and 21% ( $p < 0.05$ ) lower in the everolimus group than in the control group, respectively.

### 3.3 | Everolimus reduces hepatic fat accumulation and RWAT and EWAT adipocyte size

By performing morphometric analysis, we discovered that the mice treated with everolimus had markedly reduced-fat concentration in the liver, RWAT, and EWAT compared with control mice, as revealed using hematoxylin-eosin staining (Figure 4A). These

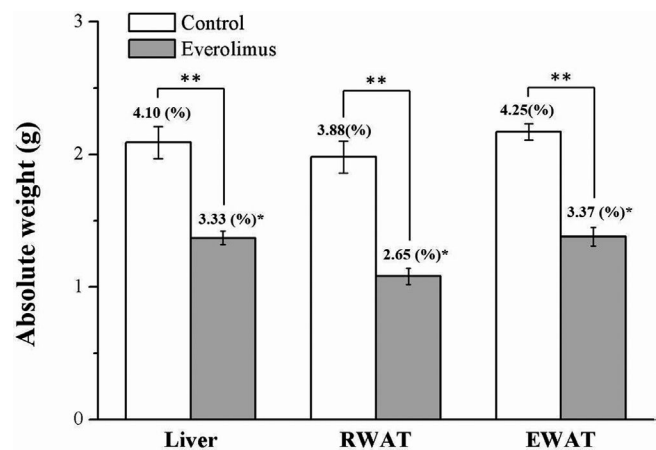


**FIGURE 3** Changes in absolute liver and EWAT- and RWAT-pad weights (presented as % of the body weight) in the control and everolimus-treated HFD-fed mice over 56 treatment days. All values are presented as means  $\pm$  SEMs, and  $n = 10$  for all groups. \* $p < 0.05$ , significant; \*\* $p < 0.01$ , highly significant. RWAT, retroperitoneal white adipose tissue; EWAT, epididymal white adipose tissue

findings indicated that everolimus prevented fat accumulation in the liver; this probably reduced fat pad hypertrophy. We also assessed how everolimus affected fatty liver scores (Figure 4B) as well as RWAT and EWAT adipocyte size (Figure 4C,D, respectively). Significant between-group differences were discovered.

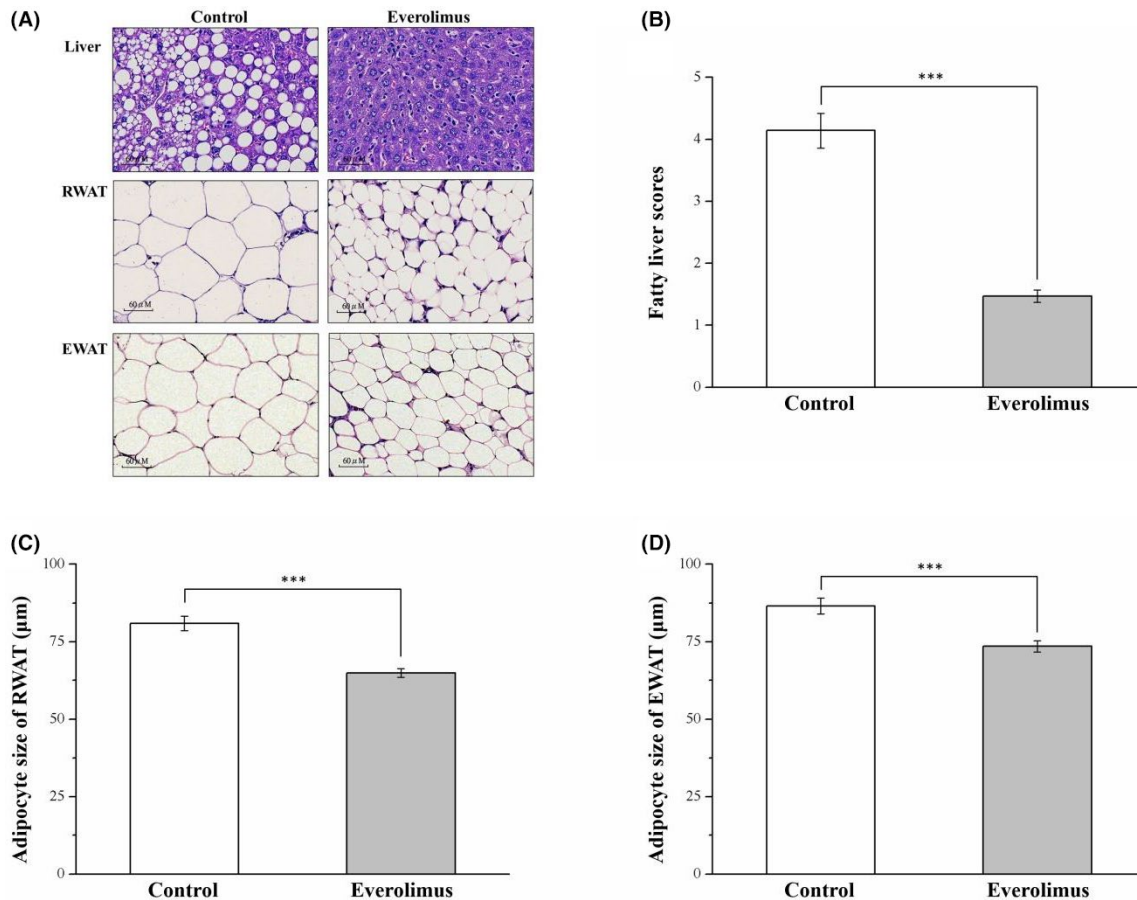


**FIGURE 4** (A) Photomicrographs of hematoxylin–eosin-stained liver, RWAT, and EWAT sections (magnification, 200×). Changes in (B) fatty liver scores and (C) RWAT and (D) EWAT adipocyte cellularities in the control and everolimus-treated HFD-fed mice over 56 treatment days. All values are presented as means  $\pm$  SEMs, and  $n = 10$  for all groups. \*\*\* $p < 0.001$ , extremely significant. Scale bar = 60  $\mu\text{m}$ ; RWAT, retroperitoneal white adipose tissue; EWAT, epididymal white adipose tissue

Compared with the controls, the everolimus group had an approximately threefold reduction in fatty liver score ( $p < 0.001$ ). The staining revealed that the everolimus group had consistently smaller adipocytes on average, with a mean reduction of 21% and 19%, respectively, in the sizes of EWAT and RWAT pads (both  $p < 0.01$ ). These results concurred with the observed lower fat pad weights of the two groups.

### 3.4 | Everolimus reduces the number of large adipocytes

We discovered that the adipocytes were all smaller in the everolimus group than in the control group. Compared with the control group, the everolimus group had a higher percentage of adipocytes that were 0–40 and 40–80  $\mu\text{m}$  in diameter in the RWAT (both  $p < 0.05$ ) and EWAT ( $p < 0.05$  and  $p < 0.01$ , respectively, but a lower percentage of adipocytes that were 80–120  $\mu\text{m}$  ( $p < 0.01$ ) and >120  $\mu\text{m}$  ( $p < 0.05$ ) in diameter (Table 1). Everolimus treatment thus resulted in fewer large adipocytes, which explains the decrease in fat pad weight.

**TABLE 1** Effect of everolimus on adipocyte size distribution in the control and everolimus-treated HFD-fed mice over the 56 treatment days

Variable	Control	Everolimus
<b>RWAT</b>		
Adipocyte diameter		
0–40 $\mu\text{m}$ (%)	0 $\pm$ 0	14.57 $\pm$ 0.92*
40–80 $\mu\text{m}$ (%)	50.44 $\pm$ 5.44	64.15 $\pm$ 3.21*
80–120 $\mu\text{m}$ (%)	42.89 $\pm$ 4.63	20.05 $\pm$ 3.69**
>120 $\mu\text{m}$ (%)	6.69 $\pm$ 0.81	1.23 $\pm$ 0.03*
<b>EWAT</b>		
Adipocyte diameter		
0–40 $\mu\text{m}$ (%)	2.04 $\pm$ 0.02	10.37 $\pm$ 0.91*
40–80 $\mu\text{m}$ (%)	35.72 $\pm$ 2.56	58.29 $\pm$ 4.84**
80–120 $\mu\text{m}$ (%)	52.15 $\pm$ 4.91	28.84 $\pm$ 3.15**
>120 $\mu\text{m}$ (%)	10.09 $\pm$ 0.06	2.51 $\pm$ 0.02*

Abbreviations: EWAT, epididymal white adipose tissue; RWAT, retroperitoneal white adipose tissue.

Significant at \* $p < 0.05$ , and highly significant at \*\* $p < 0.01$ ;  $n = 10$  for all groups.

### 3.5 | Everolimus reduces serum and hepatic triglyceride levels and nonalcoholic fatty liver disease-related protein levels but increases serum FA levels

As shown in Figure 5A, we found lower levels of blood triglyceride, a metabolic syndrome index, in the everolimus group than in the vehicle controls ( $p < 0.01$ ). We also examined the direct effects of everolimus on triglyceride accumulation patterns in the liver. The everolimus group exhibited decreased triglyceride accumulation resulting in approximately 53% lower hepatic triglyceride level than that of the vehicle control mice ( $p < 0.01$ ; Figure 5B). Everolimus-treated obese mice had increased serum FA levels ( $p < 0.01$ ; Figure 5C), which are linked to lipolysis and energy metabolism. To further characterize the molecular effects of everolimus on fatty liver, we measured the expression of fatty liver markers and thus the effect of everolimus on the regulation of lipid synthesis and homeostasis. The markers assessed were FASN, adiponectin, PNPLA3, and AMPK (Figure 5D). FASN is crucial to triglyceride synthesis and lipid homeostasis.<sup>23</sup> Western blotting of liver tissue revealed significantly lower FASN

expression ( $p < 0.01$ ) in the everolimus group than in the control group (Figure 5E). Western blotting was performed to analyze mouse liver adiponectin and PNPLA3, which are opposite markers and pathologically characterized by lipogenesis regulation in obesity, cardiovascular disease, and nonalcoholic fatty liver disease.<sup>23,34</sup> Compared with the control group, the everolimus group had dramatically increased adiponectin expression ( $p < 0.01$ ; Figure 5F) and decreased PNPLA3 expression in the liver ( $p < 0.05$ , Figure 5G) after the 56 days of everolimus treatment on an HFD. Liver-specific activation of AMPK reduced lipogenesis *in vivo* and played a major role in metabolic pathway integration due to energy demand.<sup>23</sup> We further discovered higher AMPK phosphorylation ( $p < 0.05$ ; Figure 5H) and AMPK expression ( $p < 0.05$ ; Figure 5I) in the everolimus group.

### 3.6 | Everolimus impairs glucose tolerance

IPGTT was conducted on the 2 HFD groups to determine the influence of everolimus treatment on glucose homeostasis. Notably,

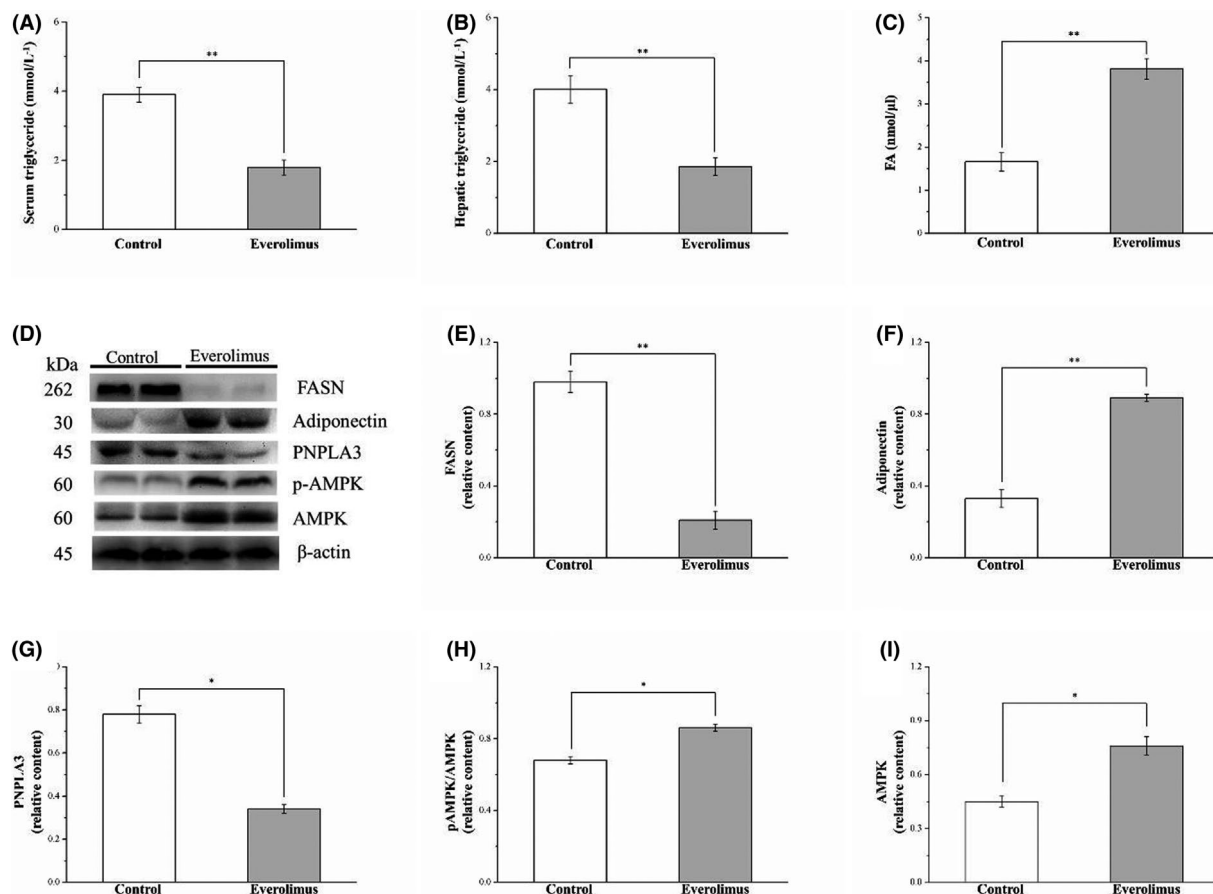


**FIGURE 5** Changes in (A) serum triglyceride levels and (B) hepatic triglyceride, (C) FA levels (E) FASN, (F) adiponectin, (G) PNPLA3, (H) phospho-AMPK and (I) AMPK levels in the control and everolimus-treated HFD-fed mice over 56 treatment days. (D) Western blot for FASN, adiponectin, PNPLA3, phospho-AMPK, and AMPK. All values are presented as means  $\pm$  SEMs, and  $n = 10$  for all groups. \* $p < 0.05$ , significant; \*\* $p < 0.01$ , highly significant. FA, fatty acid; FASN, fatty acid synthase; PNPLA3, patatin-like phospholipase domain-containing 3; AMPK, adenosine monophosphate-activated protein kinase

everolimus treatment increased fasting blood glucose levels ( $p < 0.05$ ) and exacerbated glucose intolerance, as indicated by the IPGTT data in Figure 6A. However, everolimus treatment significantly increased fasting blood glucose level at 30 ( $p < 0.05$ ), 60 ( $p < 0.001$ ), 90 ( $p < 0.01$ ), and 120 ( $p < 0.001$ ) min after glucose injection; the everolimus group had a 37% higher blood glucose level after 120 min compared with that just before the i.p. glucose injection ( $p < 0.01$ ). In addition, compared with that in the control group, the AUC for the 120-min study period was 1.5-fold higher in the everolimus group; this was a significant difference (Figure 6B). A blood glucose level higher than 8 mmol/L was used to define glucose intolerance at 120 min after i.p. glucose injection, and a significant percentage of the everolimus group mice were discovered to have glucose intolerance ( $p < 0.001$ ; Figure 6C). However, their serum insulin levels ( $p < 0.05$ ) were higher than those of the control mice (Figure 6D). We then investigated the enhancement of hepatic IR by analyzing the effect of hepatic gluconeogenic enzymes, such as *PEPCK*, on hepatic mRNA content in the treated mice.<sup>35</sup> The treated obese mice exhibited increases in *PEPCK* mRNA levels linked to the attenuation of glucose homeostasis (Figure 6E). Thus, the everolimus-treated obese mice had exacerbated DM symptoms: poorer hyperinsulinemia and hyperglycemia as well as glucose intolerance.

### 3.7 | Everolimus reduces IS by altering Akt and GLUT4 expression in HFD-induced obese mice

The IR of the mice with HFD-induced obesity was further increased and their insulin insensitivity exacerbated by chronic

everolimus administration, as revealed by the significant changes in the HOMA-IR (Figure 7A) and ISI (Figure 7B), respectively. The HOMA-IR of the everolimus-treated mice was 1.9-fold higher than that of the control mice ( $p < 0.05$ ). Furthermore, the ISI of HFD-fed mice receiving everolimus treatment was lower than that of the control animals ( $p < 0.05$ ). After everolimus treatment, we attempted to characterize the mechanisms underlying the reduced glucose homeostasis in the HFD-fed mice by evaluating Akt phosphorylation and GLUT4 expression levels in muscle tissues (Figure 7C). Phospho-Akt (Figure 7D) and GLUT4 (Figure 7E) expression was significantly lower in the everolimus group than in the control group ( $p < 0.05$ ). To identify how the mTOR pathway is inhibited after mTOR inhibitor administration, the influence of everolimus on mTOR signaling was investigated. As hypothesized, everolimus administration resulted in a dramatic reduction of mTOR ( $p < 0.01$ ; Figure 7F) and S6 K1 phosphorylation ( $p < 0.01$ ; Figure 7G). S6 K1 is an mTOR downstream target and specific mTOR activity marker crucial to DM development.<sup>6,14</sup> Thus, we speculate that everolimus may exacerbate hyperglycemia due to the reduction of insulin signaling in the muscle.

### 3.8 | Everolimus reduces serum FGF21 and increases serum TNF- $\alpha$ and IL-1 $\beta$ expression in obese mice

Next, we determined whether the effect of everolimus on FGF21, TNF- $\alpha$ , and IL-1 $\beta$  expression would be modulated in mice with HFD-induced hyperglycemia. FGF21 is a superior biomarker to other adipokines in predicting incident DM linked to improved glucose

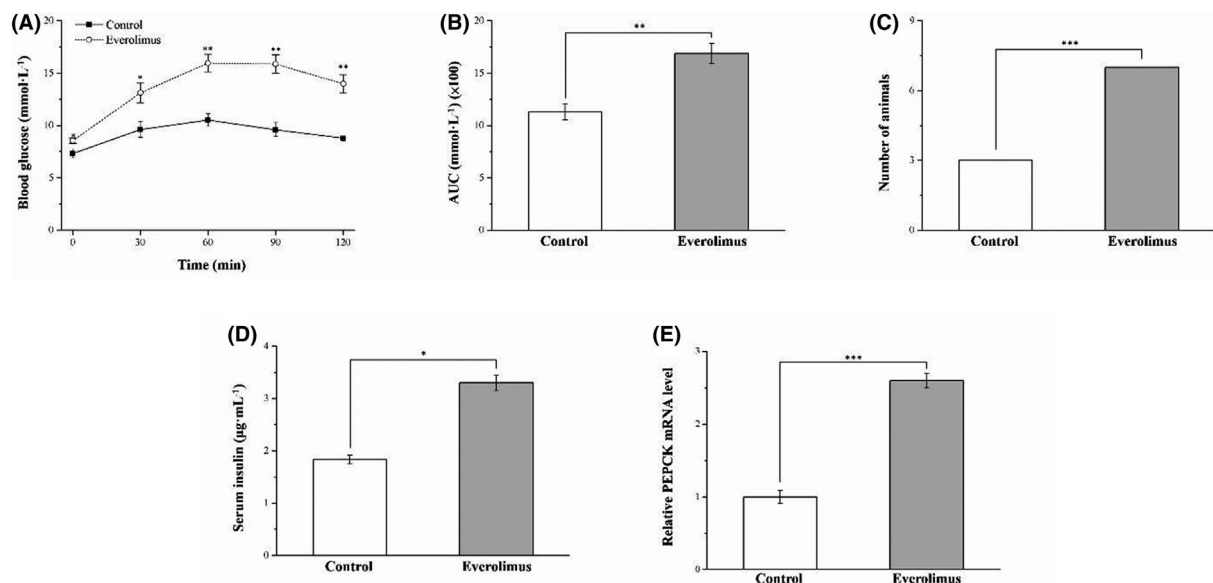


**FIGURE 6** Changes in (A) IPGTT curve, (B) AUC over 120 min after glucose injection, (C) glucose intolerance criterion (Fisher's exact test), (D) serum insulin level and (E) hepatic *PEPCK* mRNA levels in the control and everolimus-treated HFD-fed mice over 56 treatment days. All values are presented as means  $\pm$  SEMs, and  $n = 10$  for all groups. \* $p < 0.05$ , significant; \*\* $p < 0.01$ , highly significant; \*\*\* $p < 0.001$ , extremely significant. IPGTT, intraperitoneal glucose tolerance test; AUC, area under the glucose tolerance curve; PEPCK, phosphoenolpyruvate carboxy kinase



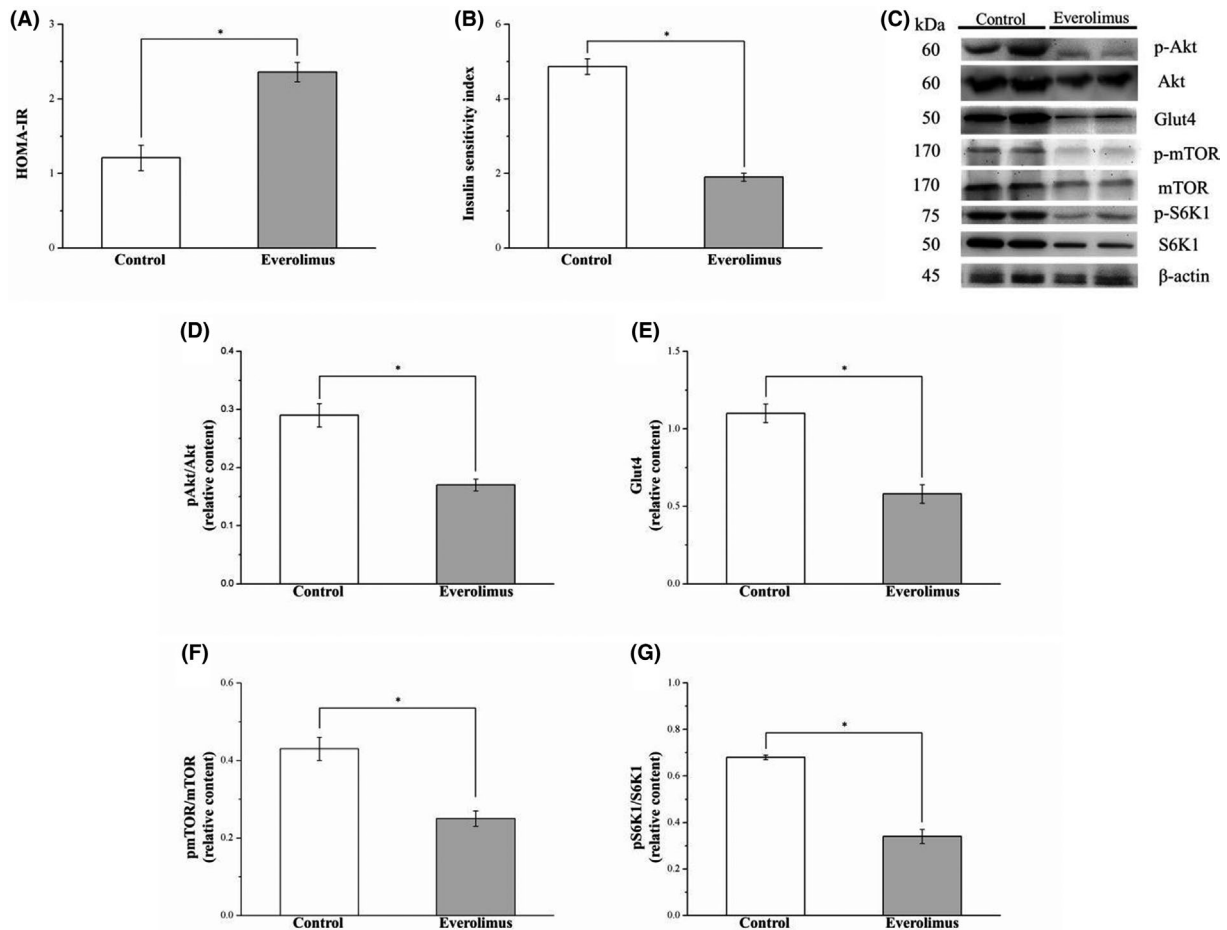


**FIGURE 7** Changes in (A) HOMA-IR, (B) ISI, and gastrocnemius muscle expression of (D) phospho-Akt, (E) GLUT4, (F) phospho-mTOR, and (G) phospho-S6 K1 in the control and everolimus-treated HFD-fed mice over 56 treatment days. (C) Western blot for phospho-Akt, GLUT4, phospho-mTOR, mTOR, phospho-S6 K1, and S6 K1. All values are presented as means  $\pm$  SEMs, and  $n = 10$  for all groups. \* $p < 0.05$ , significant. GLUT4, glucose transporter 4; mTOR, mammalian target of rapamycin; S6 K1, S6 ribosomal protein kinase 1

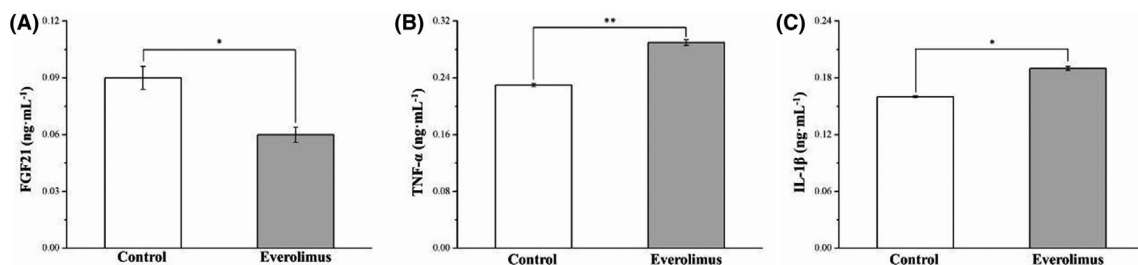


**FIGURE 8** Changes in serum (A) FGF21, (B) TNF- $\alpha$ , and (C) IL-1 $\beta$  levels in the control and everolimus-treated HFD-fed mice over 56 treatment days. All values are presented as means  $\pm$  SEMs, and  $n = 10$  for all groups. Significant at \* $p < 0.05$ , and highly significant at \*\* $p < 0.01$ . FGF21, fibroblast growth factor 21; TNF- $\alpha$ , tumor necrosis factor- $\alpha$ ; IL-1 $\beta$ , interleukin-1 $\beta$

metabolism.<sup>23,36</sup> Compared with the control group, the everolimus group had significantly lower serum FGF21 levels than did ( $p < 0.05$ , Figure 8A), but significantly higher serum TNF- $\alpha$  and IL-1 $\beta$  levels ( $p < 0.05$ ; Figure 8B,C). Higher TNF- $\alpha$  and IL-1 $\beta$  can contribute strongly to IR development and type 2 DM pathogenesis.<sup>37</sup> Our findings revealed that alterations in serum FGF21 and cytokine levels by everolimus were predominantly the result of inhibited mTOR pathway signal transduction in obese mice with IR.

## 4 | DISCUSSION

In this study, the effects of continual everolimus treatment in mice fed HFD over 12 weeks to induce obesity were analyzed. The findings revealed effects on body weight, fat, and composition; adipocyte size; fatty liver score; energy metabolism; and glucose homeostasis. Concomitantly, the everolimus group was demonstrated to consume more food but weigh less due to having less body fat. Everolimus

treatment did however cause increased blood glucose level when glucose was injected. The everolimus group of hyperglycemic mice were discovered to have worsened glucose intolerance and be less sensitive to insulin despite having higher serum insulin level.

HFDs contribute to obesity development and increases viscera fat accumulation. Interestingly, everolimus treatment of mice fed HFD for 12 weeks resulted in lower body weight, liver weight, and RWAT and EWAT pad weights than in the control group. Therefore, RWAT and EWAT loss may have occurred in the everolimus group because of decreases in adipocyte size, which we attributed to everolimus inhibiting the part of the mTOR pathway corresponding to cell proliferation and growth. One study found that body fat loss may be due to increases in energy expenditure through mTOR pathway inhibition.<sup>28</sup> We also confirmed that everolimus treatment could attenuate FSAN expression but enhance that of adiponectin in mice with HFD-induced obesity. FSAN and adiponectin are involved in fat accumulation and adipocyte differentiation.<sup>23</sup> Furthermore, we suggest that everolimus attenuates obesity resulting from excess caloric intake (compared with similarly fed controls), indicating that everolimus can promote fat combustion.

An mTOR inhibitor mimics a starvation-like signal, which arouses the appetite and prompts food consumption,<sup>10</sup> as was found for the everolimus group. Considerable evidence supports the role of leptin in food intake control by regulating appetite.<sup>6</sup> This study demonstrated that everolimus pharmacologically inhibits mTOR, and this effect lowers the leptin level, weakening leptin's anorectic effect. Conversely, clinical use of everolimus caused appetite loss and anorexia in patients with advanced solid tumors.<sup>38</sup> We hypothesized that the difference may have been due to appetite loss in patients with cancer and undergoing chemotherapy, linking to nutritional status and quality of life. Given these observations, everolimus is currently the most useful compound in the study of the effects on food intake control through mTOR signaling, thereby affecting energy balance.

We also revealed that the treated obese mice had lower fatty liver scores in histopathological examinations. Moreover, we confirmed that everolimus treatment attenuated FSAN and PNPLA3 expression in the HFD-induced obese mice. FSAN and PNPLA3 are involved in de novo lipogenesis and fat accumulation in the liver.<sup>23,39</sup> This result was also observed for knockout of S6K1, a major mTOR downstream signaling molecule, in mice.<sup>5</sup> In summary, everolimus could help prevent nonalcoholic fatty liver disease and adipocyte hypertrophy through the mTOR/S6K1 signaling pathway in mice, thus, everolimus can prevent obesity resulting from excess caloric intake.

We next investigated adiponectin, which regulates energy expenditure and metabolism through its direct activation of AMPK.<sup>23,40</sup> Their actions achieve the ultimate control of AMPK activity in liver and adipose tissue, thus reducing blood triacylglycerol levels and preventing triglyceride accumulation.<sup>41</sup> These observations are consistent with findings regarding everolimus treatment in reducing serum triglyceride levels and alleviating hepatosteatosis with triacylglycerol accumulation by enhancing AMPK phosphorylation. However, some studies have identified

hyperlipidemia as a common side effect of everolimus in humans.<sup>42,43</sup> mTOR inhibition has been observed to lead to increased fatty acid  $\beta$ -oxidation in hepatocytes and skeletal muscles and reduce the gene expression of lipogenic enzymes, such as acetyl-CoA carboxylase and stearyl-CoA desaturase. The pathogenesis of the mTOR inhibitor dyslipidemia remains unclear because dyslipidemia has not been addressed as a primary endpoint, and information pertinent to interpreting dyslipidemia incidence has not been provided in most studies.<sup>3</sup> Thus, we propose that weight gain and adipocyte accumulation reduction were considerably greater in the everolimus-treated HFD-fed mice because everolimus inhibited mTOR by increasing AMPK expression, thereby suppressing excess energy intake.

mTOR inhibitor may increase the fasting glucose level, contributing to type 2 DM pathogenesis by alleviating glucose tolerance.<sup>10,14,44</sup> According to evidence on everolimus in breast cancer, hyperglycemia is one of the most common high-grade adverse events,<sup>20</sup> moreover, everolimus induced hyperglycemia by increasing basal hepatic glucose production in diabetic and nondiabetic patients.<sup>45</sup> Our findings for everolimus-treated obese mice are consistent with previous findings regarding the exacerbation of glucose intolerance. We performed an IPGTT, which indicated that the everolimus-treated mice exhibited notable deterioration in glucose tolerance. This observation can be explained by the increased *PEPCK* mRNA levels and decreased muscle Akt phosphorylation and GLUT4 expression noted in the everolimus-treated mice on an HFD. All the aforementioned results show that everolimus-treated HFD-fed mice exhibit severe hyperglycemia and suppressed IS, even when they are hyperinsulinemic. Thus, our findings indicate that impairment of muscle glucose uptake due to everolimus-induced chronic mTOR inhibition can occur through additional mechanisms.

Previous clinical studies on the recipients of kidney allografts, however, have noted that everolimus treatment, which alleviates hyperglycemia, did not increase insulin requirements and could improve renal function.<sup>19,46</sup> Moreover, everolimus administration at 1 mg/kg three times per week for 16 weeks in mice fed a fast-food diet improved IR.<sup>21</sup> This disagrees with our finding that everolimus resulted in dramatically poorer glucose tolerance and lower ISI. The apparent discrepancy in the effects of everolimus is likely due to differences that occur from dosing titration; frequency and period of administration should be of prime concern for such studies. Conversely, reports have indicated everolimus, similarly to the antidiabetic drug metformin, has a Janus Bifrons effect on glucose metabolism, which can be represented as a U-shaped curve; glucose parameters are adversely affected according to the degree to which mTOR is inhibited. Furthermore, both extremities of the U-shaped curve indicate a considerably worsened glucose metabolic profile with poor IR.<sup>3,47</sup> In addition, the everolimus-treated mice were discovered to have increased serum insulin level—corroborating the previously reported hepatic insulin clearance defects.<sup>6</sup> This finding, together with those of another study, suggests that rapamycin treatment's positive or adverse effects on metabolism, whether considering those with DM or who are prediabetic, are the consequence of mTOR inhibition

interacting with insulin level in the individual model.<sup>48</sup> Overall, the evidence appears to indicate that everolimus systemically inhibits mTOR signaling, potentially altering insulin signaling and glucose homeostasis, possibly subsequent to IR—as demonstrated by the increased serum insulin levels.

Scholars have observed mTOR pathway dysregulation in several neoplastic and inflammatory human diseases.<sup>49,50</sup> Our finding showed that obese mice treated with everolimus had increased TNF- $\alpha$  and IL-1 $\beta$  levels. This was similar to the finding that inhibited mTOR signaling induces the expression of cytokines including PDGF, TNF- $\alpha$ , MIP-1 TGF- $\beta$ , MCP-1, IL-1, IL-3, and IL-6 in a mouse model<sup>51</sup> and in macrophages.<sup>52</sup> This observation may be explained by the treatment duration of mTOR inhibitor blocks or the lack of effect on the proliferative response of cell lines to a variety of hematopoietic growth factors, such as granulocyte colony-stimulating factor, granulocyte-macrophage colony-stimulating factor, IL-3, and IL-6.<sup>53</sup> This suggests that the immunosuppressant everolimus affects cytokine levels but not steady-state homeostasis in vivo related to health or patient condition.

Mice on an HFD treated with everolimus had lower FGF21 levels than did control mice; this result reveals that everolimus ameliorates glucose homeostasis in obesity and DM models.<sup>54</sup> In addition, TNF- $\alpha$  and IL-1 $\beta$  lead to the pathological and physiological development of type-2-DM-associated IR by impairing insulin signaling.<sup>55,56</sup> Furthermore, in vitro, FGF21 inhibited IL-1, IL-6, and TNF- $\alpha$  release.<sup>57</sup> This suggests that the lower serum FGF21 level of the everolimus-treated mice did not attenuate the serum levels of IL-1 $\beta$  and TNF- $\alpha$ , this may have contributed to the exacerbated IR.

In conclusion, we discovered that continual administration of everolimus to obese HFD-fed mice led to a reduction in body weight gain, food efficiency, liver and fat tissue weight, serum triglyceride level, hepatic triglyceride level, fatty liver score, and adipocyte size despite these mice eating more than the controls. Moreover, administering everolimus to obese mice resulted in exacerbated hyperglycemia and impairment of glucose tolerance. A decrease in the expression of skeletal muscle Akt phosphorylation and GLUT4 may have contributed to these alterations in glucose metabolism. Furthermore, everolimus caused DM symptoms to develop in the mice, and the HFD accelerated the impairment of glucose homeostasis. Everolimus may thus be effective when treating transplant patients experiencing organ rejection. However, use for a long period may result in the adverse effects associated with DM even if it does prevent obesity.

## ACKNOWLEDGMENTS

The authors thank LiTzung Biotechnology, Kaohsiung, Taiwan, for providing pathological assistance for this study. This study was supported in part by Grant 109D1-100A-A-A2 from the Ministry of Education, Executive Yuan (Taiwan), the Show Chwan Memorial Hospital (Taiwan) (SRD108025), the Chang Gung Memorial Hospital (Taiwan) (CMRPG5J0191), the Taichung Veterans General Hospital (Taiwan) and National Chung-Hsing University (Taiwan) (TCVGH-NCHU-1097612), and the National Chiayi University (Taiwan)

(108A3-129, 108A3-147, and 108A3-161). In addition, the authors thank Wallace Academic Editing (ISO 9001: 2015 certified for quality) for the English edition.

## CONFLICT OF INTEREST

The authors declare no conflicts of interest.

## AUTHORS' CONTRIBUTIONS

P. H. H., C. M. W., C. F. W., H. K. S., and H. J. L. carried out testing analysis and interpretation of data for the work. G. R. C. contributed to the study design and advised on translational aspects of experiments. G. R. C. and T. P. C. supervised all experiments, advised on statistical analysis and co-wrote the manuscript.

## DATA AVAILABILITY STATEMENT

The data presented in this study are available on request from the corresponding author.

## ORCID

Geng-Ruei Chang  <https://orcid.org/0000-0003-0577-3339>

## REFERENCES

- Macaskill EJ, Bartlett JMS, Sabine VS, et al. The mammalian target of rapamycin inhibitor everolimus (RAD001) in early breast cancer: results of a pre-operative study. *Breast Cancer Res Treat.* 2011;128:725-734.
- Maráz A, Csejtei A, Kocsis J, et al. Assessment of the role of everolimus therapy in patients with renal cell carcinoma based on daily routine and recent research results. *Pathol Oncol Res.* 2019;25:149-156.
- Morviducci L, Rota F, Rizza L, et al. Everolimus is a new anti-cancer molecule: metabolic side effects as lipid disorders and hyperglycemia. *Diabetes Res Clin Pract.* 2018;143:428-431.
- Schmid P, Zaiss M, Harper-Wynne C, et al. Fulvestrant plus vistusertib vs fulvestrant plus everolimus vs fulvestrant alone for women with hormone receptor-positive metastatic breast cancer: the manta phase 2 randomized clinical trial. *JAMA Oncol.* 2019;5:1556-1563.
- Um SH, Frigerio F, Watanabe M, et al. Absence of S6K1 protects against age- and diet-induced obesity while enhancing insulin sensitivity. *Nature.* 2004;431:200-205.
- Chang GR, Chiu YS, Wu YY, Lin YC, Hou PH, Mao FC. Rapamycin impairs HPD-induced beneficial effects on glucose homeostasis. *Br J Pharmacol.* 2015;172:3793-3804.
- Kezic A, Popovic L, Lalic K. mTOR inhibitor therapy and metabolic consequences: where do we stand? *Oxid Med Cell Longev.* 2018;2018:2640342.
- Tzatsos A, Kandror KV. Nutrients suppress phosphatidylinositol 3-kinase/Akt signaling via raptor-dependent mTOR-mediated insulin receptor substrate 1 phosphorylation. *Mol Cell Biol.* 2006;26:63-76.
- Chang GR, Chen WK, Hou PH, Mao FC. Isoproterenol exacerbates hyperglycemia and modulates chromium distribution in mice fed with high fat diet. *J Trace Elem Med Biol.* 2017;44:315-321.
- Chang GR, Chiu YS, Wu YY, et al. Rapamycin protects against high fat diet-induced obesity in C57BL/6J mice. *J Pharmacol Sci.* 2009;109:496-503.
- Tsai HP, Hou PH, Mao FC, et al. Risperidone exacerbates glucose intolerance, nonalcoholic fatty liver disease, and renal impairment in obese mice. *Int J Mol Sci.* 2021;22:409.

12. Schriever SC, Deutsch MJ, Adamski J, Roscher AA, Ensenauer R. Cellular signaling of amino acids towards mtorc1 activation in impaired human leucine catabolism. *J Nutr Biochem*. 2013;24:824-831.
13. Wiperman MF, Montrose DC, Gotto AM Jr, Hajjar DP. Mammalian target of rapamycin: a metabolic rheostat for regulating adipose tissue function and cardiovascular health. *Am J Pathol*. 2019;189:492-501.
14. Chang GR, Wu YY, Chiu YS, et al. Long-term administration of rapamycin reduces adiposity, but impairs glucose tolerance in high-fat diet-fed KK/HIJ mice. *Basic Clin Pharmacol Toxicol*. 2009;105:188-198.
15. Reifsnnyder PC, Ryzhov S, Flurkey K, et al. Cardioprotective effects of dietary rapamycin on adult female C57BLKS/J-Leprdb mice. *Ann N Y Acad Sci*. 2018;1418:106-117.
16. Matsumoto Y, Hof A, Baumlin Y, Hof RP. Differential effect of cyclosporine A and SDZ RAD on neointima formation of carotid allografts in apolipoprotein E-deficient mice. *Transplantation*. 2003;76:1166-1170.
17. Lorber MI, Mulgaonkar S, Butt KM, et al. Everolimus versus mycophenolate mofetil in the prevention of rejection in de novo renal transplant recipients: a 3-year randomized, multicenter, phase III study. *Transplantation*. 2005;80:244-252.
18. Vitko S, Margreiter R, Weimar W, et al. Three-year efficacy and safety results from a study of everolimus versus mycophenolate mofetil in de novo renal transplant patients. *Am J Transplant*. 2005;5:2521-2530.
19. Ayala M, Morales J, Fierro A, Herzog C, Calabran L, Buckel E. Metabolic changes following conversion from an anticalcineurin-based therapy to an everolimus-based one: a single-center experience. *Transplant Proc*. 2008;40:3265-3269.
20. Pizzuti L, Marchetti P, Natoli C, et al. Fasting glucose and body mass index as predictors of activity in breast cancer patients treated with everolimus-exemestane: the everext study. *Sci Rep*. 2017;7:10597.
21. Love S, Mudasir MA, Bhardwaj SC, Singh G, Tasduq SA. Long-term administration of tacrolimus and everolimus prevents high cholesterol-high fructose-induced steatosis in C57BL/6J mice by inhibiting de-novo lipogenesis. *Oncotarget*. 2017;8:113403-113417.
22. Lin C, Chen PW, Chen WY, Sun CC, Mao FC. Glucagon and insulin have opposite effects on tissue chromium distribution in an obese mouse model. *J Diabetes Investig*. 2013;4:528-532.
23. Wu CF, Hou PH, Mao FC, et al. Mirtazapine reduces adipocyte hypertrophy and increases glucose transporter expression in obese mice. *Animals*. 2020;10:1423.
24. Brandt C, Hillmann P, Noack A, et al. The novel, catalytic MTORC1/2 inhibitor PQR620 and the PI3K/MTORC1/2 inhibitor PQR530 effectively cross the blood-brain barrier and increase seizure threshold in a mouse model of chronic epilepsy. *Neuropharmacology*. 2018;140:107-120.
25. Ayril-Kaloustian S, Gu J, Lucas J, et al. Hybrid inhibitors of phosphatidylinositol 3-kinase (PI3K) and the mammalian target of rapamycin (mTOR): design, synthesis, and superior antitumor activity of novel wortmannin-rapamycin conjugates. *J Med Chem*. 2010;53:452-459.
26. Kurdi A, Roth L, Van der Veken B, et al. Everolimus depletes plaque macrophages, abolishes intraplaque neovascularization and improves survival in mice with advanced atherosclerosis. *Vascul Pharmacol*. 2019;113:70-76.
27. Majewski M, Korecka M, Joergensen J, et al. Immunosuppressive TOR kinase inhibitor everolimus (RAD) suppresses growth of cells derived from posttransplant lymphoproliferative disorder at allograft-protecting doses. *Transplantation*. 2003;75:1710-1717.
28. Mueller MA, Beutner F, Teupser FD, Ceglarek U, Thiery J. Prevention of atherosclerosis by the mTOR inhibitor everolimus in LDLR<sup>-/-</sup> mice despite severe hypercholesterolemia. *Atherosclerosis*. 2008;198:39-48.
29. Suyani E, Derici UB, Sahin T, et al. Effects of everolimus on cytokines, oxidative stress, and renal histology in ischemia-reperfusion injury of the kidney. *Ren Fail*. 2009;31:698-703.
30. Zhao N, Li X, He X, Qiu Y, Zhu L, Qi F. Interleukin-15 gene therapy and the mammalian target of rapamycin inhibitor everolimus inhibit the growth of metastatic breast cancer. *J Gene Med*. 2013;15:366-374.
31. London E, Castonguay TW. High fructose diets increase 11 $\beta$ -hydroxysteroid dehydrogenase type 1 in liver and visceral adipose in rats within 24-h exposure. *Obesity*. 2011;19:925-932.
32. Ahn SW, Gang GT, Tadi S, et al. Phosphoenolpyruvate carboxylase and glucose-6-phosphatase are required for steroidogenesis in testicular Leydig cells. *J Biol Chem*. 2012;287:41875-41887.
33. Chang GR, Hou PH, Chen WK, Lin CT, Tsai HP, Mao FC. Exercise affects blood glucose levels and tissue chromium distribution in high-fat diet-fed C57BL6 mice. *Molecules*. 2020;25:1658.
34. Finelli C, Tarantino G. What is the role of adiponectin in obesity related non-alcoholic fatty liver disease? *World J Gastroenterol*. 2013;19:802-812.
35. Lamming DW, Ye L, Katajisto P, et al. Rapamycin-induced insulin resistance is mediated by mTORC2 loss and uncoupled from longevity. *Science*. 2012;335:1638-1643.
36. Woo YC, Lee CH, Fong CHY, et al. Serum fibroblast growth factor 21 is a superior biomarker to other adipokines in predicting incident diabetes. *Clin Endocrinol*. 2017;86:37-43.
37. Jaganathan R, Ravindran R, Dhanasekaran S. Emerging role of adipocytokines in type 2 diabetes as mediators of insulin resistance and cardiovascular disease. *Can J Diabetes*. 2018;42:446-456.
38. O'Donnell A, Faivre S, Burris HA, et al. Phase I pharmacokinetic and pharmacodynamic study of the oral mammalian target of rapamycin inhibitor everolimus in patients with advanced solid tumors. *J Clin Oncol*. 2008;26:1588-1595.
39. Hou PH, Chang GR, Chen CP, et al. Long-term administration of olanzapine induces adiposity and increases hepatic fatty acid desaturation protein in female C57BL/6J mice. *Iran J Basic Med Sci*. 2018;21:495-501.
40. Kubota N, Yano W, Kubota T, et al. Adiponectin stimulates AMP-activated protein kinase in the hypothalamus and increases food intake. *Cell Metab*. 2007;6:55-68.
41. Lafontan M, Viguier N. Role of adipokines in the control of energy metabolism: focus on adiponectin. *Curr Opin Pharmacol*. 2006;6:580-585.
42. Kelsh SE, Girgis R, Dickinson M, McDermott JK. Everolimus use for intolerance or failure of baseline immunosuppression in adult heart and lung transplantation. *Ann Transplant*. 2018;23:744-750.
43. Paplomata E, Zelnak A, O'Regan R. Everolimus: side effect profile and management of toxicities in breast cancer. *Breast Cancer Res Treat*. 2013;140:453-462.
44. Ejaz A, Mitterberger MC, Lu Z, et al. Weight loss upregulates the small gtpase diras3 in human white adipose progenitor cells, which negatively regulates adipogenesis and activates autophagy via Akt-mTOR inhibition. *EBioMedicine*. 2016;6:149-161.
45. Tanimura J, Nakagawa H, Tanaka T, et al. The clinical course and potential underlying mechanisms of everolimus-induced hyperglycemia. *Endocr J*. 2019;66:615-620.
46. Kälble F, Seckinger J, Schafer M, et al. Switch to an everolimus-facilitated cyclosporine A sparing immunosuppression improves glycemic control in selected kidney transplant recipients. *Clin Transplant*. 2017;31:e13024.
47. Fiebrich HB, Siemerink EJ, Brouwers AH, et al. Everolimus induces rapid plasma glucose normalization in insulinoma patients by effects on tumor as well as normal tissues. *Oncologist*. 2011;16:783-787.
48. Reifsnnyder PC, Flurkey K, Te A, Harrison DE. Rapamycin treatment benefits glucose metabolism in mouse models of type 2 diabetes. *Aging*. 2016;8:3120-3130.

49. Balato A, Caprio RD, Lembo S, et al. Mammalian target of rapamycin in inflammatory skin conditions. *Eur J Inflamm*. 2014;12:341-350.
50. Pinto A, Jahn A, Immohr MB, et al. Modulation of immunologic response by preventive everolimus application in a rat CPB model. *Inflammation*. 2016;39:1771-1782.
51. Kim SH, Lee JE, Yang SH, Lee SW. Induction of cytokines and growth factors by rapamycin in the microenvironment of brain metastases of lung cancer. *Oncol Lett*. 2013;5:953-958.
52. Baker AK, Wang R, Mackman N, Luyendyk NP. Rapamycin enhances LPS induction of tissue factor and tumor necrosis factor-alpha expression in macrophages by reducing IL-10 expression. *Mol Immunol*. 2009;46:2249-2255.
53. Quesniaux VF, Wehrli S, Steiner C, et al. The immunosuppressant rapamycin blocks in vitro responses to hematopoietic cytokines and inhibits recovering but not steady-state hematopoiesis in vivo. *Blood*. 1994;84:1543-1552.
54. Guridi M, Tintignac LA, Lin S, Kupr B, Castets P, Rüegg MA. Activation of mTORC1 in skeletal muscle regulates whole-body metabolism through FGF21. *Sci Signal*. 2015;8:ra113.
55. Akash MSH, Rehman K, Liaqat A. Tumor necrosis factor-alpha: role in development of insulin resistance and pathogenesis of type 2 diabetes mellitus. *J Cell Biochem*. 2018;119:105-110.
56. Fève B, Bastard JP. The role of interleukins in insulin resistance and type 2 diabetes mellitus. *Nat Rev Endocrinol*. 2009;5:305-311.
57. Liu J, Cai G, Li M, et al. Fibroblast growth factor 21 attenuates hypoxia-induced pulmonary hypertension by upregulating PPARγ expression and suppressing inflammatory cytokine levels. *Biochem Biophys Res Commun*. 2018;504:478-484.

**How to cite this article:** Chang G, Hou P, Wang C, et al. Chronic everolimus treatment of high-fat diet mice leads to a reduction in obesity but impaired glucose tolerance. *Pharmacol Res Perspect*. 2021;9:e00732. <https://doi.org/10.1002/prp2.732>